Albedo of a Dissipating Snow Cover[1]

DAVID A. ROBINSON AND GEORGE KUKLA

Lamont-Doherty Geological Observatory, Columbia University, Palisades, NY 10964

(Manuscript received 18 June 1984, in final form 29 September 1984)

ABSTRACT

Albedos of surfaces covered with 50 cm of fresh dry snow following a major U.S. East Coast storm on 11–12 February 1983 ranged from 0.20 over a mixed coniferous forest to 0.80 over open farmland. As the snow cover dissipated, albedo decreased in a quasi-linear fashion over forests. It dropped rapidly at first, then slowly, over shrubland; while the opposite was observed over farmland.

Following the melt, the albedo of snowfree surfaces ranged from 0.07 over a predominantly wet peat field to 0.20 over a field covered with corn stubble and yellow grass. The difference between snow-covered and snowfree albedo was 0.72 over the peaty field and 0.10 over the mixed forest.

Visible band (0.28–0.69 μm) reflectivities of snow-covered fields and shrubland were higher than those in the near-infrared (0.69–2.80 μm), whereas the opposite was true over mixed coniferous forests. Visible and near-infrared reflectivities were approximately equal over deciduous forests.

Data were collected in a series of low-altitude flights between 10 February and 24 March 1984 in northern New Jersey and southeastern New York with Eppley hemispheric pyranometers mounted on the wingtip of a Cessna 172 aircraft.

1. Introduction

Increases in atmospheric CO_2 and other "greenhouse" gases are expected to have a major impact on the climate of the middle latitudes in the Northern Hemisphere, due in part to snow–ice/albedo feedbacks (Ramanathan *et al.*, 1979; Robock, 1983). The land surface in this zone shows the largest annual and interannual variation in albedo, due to the formation of a seasonal snow cover (Kung *et al.*, 1964; Robock, 1980). A large portion of the earth's population resides in this region. Man's use of the land, primarily for agriculture, has resulted in extensive deforestation (Matthews, 1983). This, in turn, has resulted in significant alterations of seasonal and annual surface albedo, particularly when snow cover is present (Robinson, 1984).

McFadden and Ragotzkie (1967), Federer (1971), Berglund and Mace (1972), O'Neill and Gray (1973), Jurik and Gates (1983) and others have studied winter surface albedo in the middle latitudes. The most complete airborne research was conducted by Kung *et al.* (1964). They collected data during a series of monthly flights over Wisconsin. The major disadvantage of Kung's study was the use of a beam collector with a single calibration factor for converting beam measurements to hemispheric values. Surfaces have since been shown to have various degrees of anisotropy (e.g. Eaton and Dirmhirn, 1979; Taylor and Stowe, 1984). Anisotropy is particularly significant over snow, ice and water at high solar zenith angles.

The need for accurate surface albedos and spectral reflectivities under different snow cover conditions has grown because of the increasing sophistication of climate models (Henderson-Sellers and Wilson, 1983).

A heavy snowfall from a major East Coast storm on 11–12 February 1983 left southeastern New York and northern New Jersey covered with approximately 50 cm of snow. A three-week period of melting followed, providing an opportunity to collect shortwave albedo and spectral reflectivities over a variety of fully and partially covered snow surfaces. Daily high temperatures were above freezing following the storm, and there was no significant rain or snowfall until 2 March, when practically all of the snow cover was gone. Snow depth on flight days ranged from an average of 50 cm over forests and 43 cm in fields on 14 February to traces or patches on 3 March. The snow was wet every day after the 14th and grain size gradually increased from 0.2 mm on the 14th to 2.0 mm on the 22nd. During this 8-day period the snow albedo decreased from 0.83 to 0.60. Climatic conditions during the study period and surface conditions on flight days are further described in Tables 1 and 2.

2. Methodology

Albedo and near-infrared (NIR) hemispheric reflectivity were measured during eight flight missions between 10 February and 24 March 1983 taken along

[1] Lamont-Doherty Geological Observatory Contribution Number 3749.

TABLE 1. Climatic conditions prior to and during the study period (5 February 1983–24 March 1983). Daily high (H) and low (L) temperatures and precipitation (P) are averaged from eight NOAA Cooperative Observation stations in the vicinity of the flight region (cf. Fig. 1). Daily snowfall (SF) and snow cover (SC) are averaged from three of these stations; H and L are in °C (rounded to the nearest whole number); P in mm; SF and SC in cm; t = trace. Asterisks indicate that not all stations reported measurable values.

Date (February)	H	L	P	SF	SC	Date (March)	H	L	P	SF	SC
5	2	−9	t*	t*	t*	1	11	−1	1*	0	3*
6	−1	−10	t*	1*	t*	2	11	2	17	0	t*
7	−2	−8	14	12	13	3	13	4	t*	0	t*
8	0	−5	5*	1*	13	4	12	1	t*	t*	0
9	0	−8	t*	t*	10	5	8	1	3	0	0
10	−1	−18	0	0	10	6	8	−2	t*	0	0
11	−5	−16	1*	2*	13	7	8	2	12	0	0
12	−4	−12	32	50	61	8	7	1	5	0	0
13	1	−17	0	0	51	9	5	1	15	0	0
14	4	−14	0	0	43	10	6	2	5*	0	0
15	5	−11	0	0	38	11	5	1	9	0	0
16	7	−6	t*	0	33	12	6	0	13	1	3*
17	7	−3	1*	0	25	13	7	0	1	2	t*
18	7	0	2*	0	20	14	13	0	0	0	0
19	8	−5	0	0	18	15	16	3	t*	0	0
20	8	−8	0	0	15	16	16	0	0	0	0
21	10	−5	0	0	15	17	12	0	0	0	0
22	11	−2	0	0	13	18	7	2	3*	0	0
23	10	0	t*	0	10	19	13	5	60	0	0
24	7	−3	t*	t*	8	20	14	7	2*	0	0
25	6	−3	0	0	8	21	13	2	11*	0	0
26	4	−5	0	0	5	22	12	1	20	t	t*
27	3	−8	0	0	5	23	3	−7	t*	t	t*
28	10	−4	0	0	3*	24	5	−6	0	0	0

the flight path shown in Fig. 1. The 10 February flight documented the albedo of surfaces covered with 4-day old snow deposited prior to the major storm. Six flights from 14 February to 3 March recorded albedo with full and partial snow cover following the storm. The 24 March flight documented the albedo of completely snowfree early spring surfaces, which in our study area do not differ from snowfree winter surfaces.

A Cessna 172 aircraft was equipped with wingtip-mounted upward- and downward-facing hemispheric Eppley pyranometers which recorded shortwave (SW, 0.28–2.80 μm) and NIR (0.69–2.80 μm) radiation. The latter was done using a RG695 filter. Signals were amplified and recorded in the cabin, as were aircraft location, altitude and attitude and the sky condition. Measurements were documented with a wingtip-mounted Olympus OM-2N 35 mm camera

TABLE 2. Surface conditions on flight dates. On dates with full or partial snow cover the exposed vegetation was dry and any exposed soil was wet. Snow conditions on these dates are listed. Depth (cm) includes mean and (range). Age is days since the last measurable snowfall. Grain size is the mean for both forest and field (mm). Wetness is wet (w) (standing water and/or slushy snow) or dry (d). Field measurements were taken at the mucklands and in a deciduous forest within the region. Snow albedos (A) and reflectivities (R) were measured over a 100% snow-covered grass field at Lamont (cf. Fig. 1), except on 1 and 3 March when they were estimated (e).

Date (1983)	Depth		Age	Grain size	Wetness	A	R	
	field	forest					NIR	VIS
				Full or partial snowcover				
10 Feb	13 (0–15)	13 (10–15)	3	0.4	d	0.78	0.65	0.90
14 Feb	43 (30–55)	50 (43–55)	2	0.2	d	0.83	0.73	0.94
18 Feb	23 (18–28)	33 (23–40)	6	+1.5	w	0.75	0.60	0.90
22 Feb	13 (8–18)	13 (10–15)	10	+2.0	w	0.60	0.49	0.72
25 Feb	5 (0–10)	8 (5–10)	14	+2.0	w	0.54	0.42	0.66
1 Mar	1 (0–5)	3 (0–8)	18	+2.0	w	e0.50	e0.40	e0.60
3 Mar	0 (0–2)	0 (0–2)	20	+2.0	w	e0.50	e0.40	e0.60
				Snowfree				
24 Mar	vegetation—leafless trees, dormant grass, dry exposed soil—wet some standing water in fields							

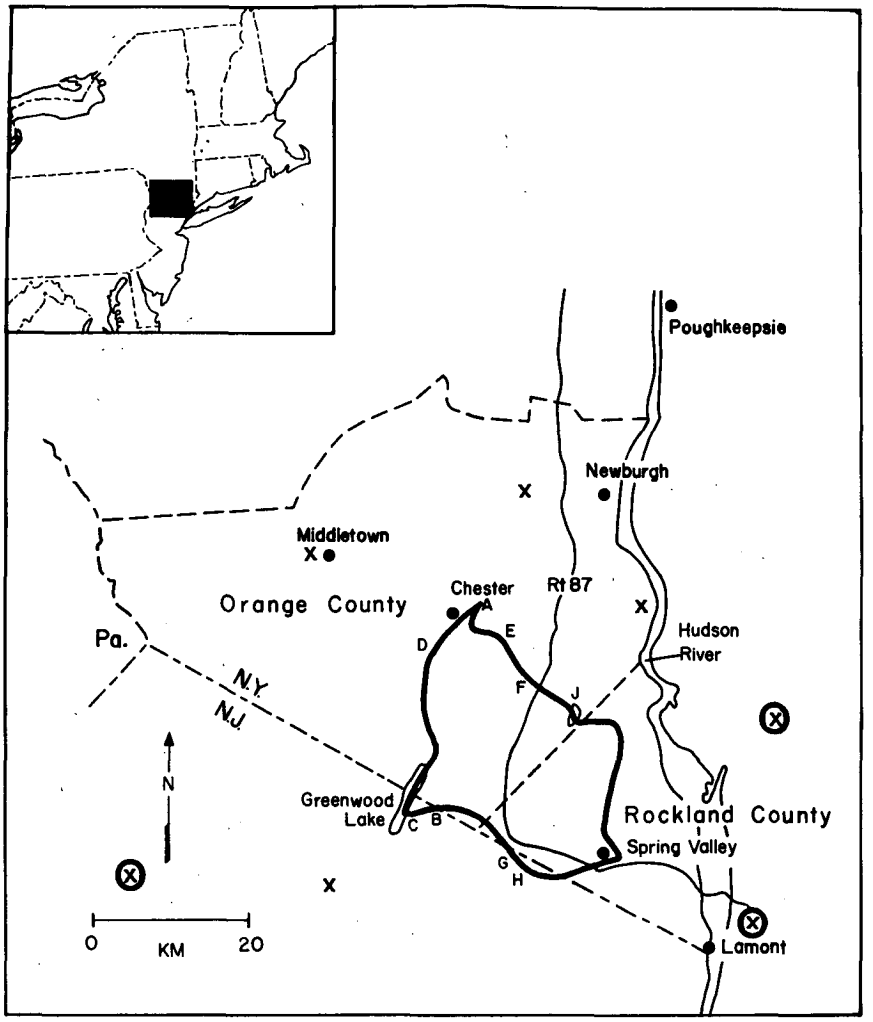

FIG. 1. Flight path (heavy line), study sites (A–H) and NOAA Cooperative Observation sites used in the investigation. Cross denotes temperature and precipitation; circled cross, temperature, precipitation and snow.

equipped with a 250 exposure bulk film pack camera back, autowinder and an Olympus 6 mm fisheye (180°) lens. At the 200 m average flight altitude, 90% of the reflected signal came from an area of approximately 0.50 km^2. Atmospheric effects on the reflected signal and the difference between incoming radiations at the airplane and on flat ground were negligible (Bauer and Dutton, 1962; Barry and Chambers, 1966).

The spectral range of measured albedo is the same as that employed by others (e.g. Kung *et al.*, 1964; Rockwood and Cox, 1978). Visible reflectance (VIS, 0.28–0.69 μm) was derived as a residual of the full band SW albedo and NIR reflectance. The fraction of the total incoming SW radiation in the NIR was measured on the ground immediately prior to and following flights in order to permit the calculation. To our knowledge, ours is the first study in which wide band NIR reflectivity has been measured in low-level flight.

On a typical 40-minute mission along the 100 km route approximately 800 albedos or NIR reflectivities were recorded. Technical limitations permitted only SW or NIR measurements to be made on a single flight; therefore, two passes over the route were made each day. Differences in solar zenith angle (Table 3) or sky conditions between flights were minor and are assumed to have negligible effects on the calculation of VIS reflectivity. Several degrees of pitch and roll in normal flight attitude had insignificant effects on the incoming signal on cloudy days. On clear days we averaged the signal over 2-minute intervals and checked the results against ground measurements made immediately prior to and following flights.

The confidence limit of flight albedo and NIR reflectivity is ±4% of the calculated value. Potential

TABLE 3. Time, solar zenith angle (SZA) in degrees and atmospheric conditions during flights: *A*–albedo flight; NIR–near-infrared flight; cloud–average fractional cloud cover; *TR*–range in transmissivity during flights; *N*–incoming radiation in the near-infrared; *D*–SW diffuse radiation reaching ground at the airport immediately prior to and following flights; Temp–surface air temperature during flights at White Plains, NY, approximately 25 km east of the center of the flight path; and e denotes estimate.

Date (1983)	Time		SZA		Cloud	*TR* (%)	*D* (%)	*N* (%)	Temp (°C)
	A	NIR	*A*	NIR					
10 Feb	1222–1304	—	55–56	—	0	69	21	50	−4
14 Feb	1225–1303	1325–1403	54–56	56–60	1.0	37–46	e85	41–45	2
18 Feb	1127–1208	1245–1325	53–54	54–55	0.1	63–73	27	49–50	7
22 Feb	1151–1232	1258–1343	51	52–55	0.1	48–69	31	46–49	11
25 Feb	1433–1510	—	59–64	—	0.9	40–65	65	50	5
1 Mar	1135–1218	1234–1319	49–50	50–51	1.0	15–30	100	41–43	9
3 Mar	1333–1412	1441–1525	51–57	58–64	0	65–70	22	49	13
24 Mar	1138–1218	1237–1320	40	41–43	0	64–72	29	50–51	3

errors would result from minor deviations from the flight path, variations in aircraft altitude, averaging of incoming radiation and precision limits of the pyranometers. Confidence limits were established by comparing data among multiple flights taken over key surfaces and by comparing aerial measurements with ground readings.

The flight route was designed to cover a wide variety of natural and man-made surfaces in a short period of time. Our report focuses on eight major surface types that were homogeneous over a broad area, assuring representative measurements, and had relatively flat topography which reduced shadowing effects. They are:

A) *Mucklands.* Dark peaty soils (histosols) of a former glacial lake bed on which onions are now grown. Eighty percent of the surface is exposed soil with a micro-relief of 10–15 cm; twenty percent is scattered sections of 0.5–1.0 m tall grass in fallow plots or along drainage ditches.

B) *Deciduous forests.* Secondary forests composed mostly of white and black oak and maple. Canopy height of the approximately 100-year old stands is 20–30 m.

C) *Mixed coniferous forests.* The study site is approximately 55% coniferous and 45% deciduous with a canopy height of 20–30 m. No extensive area of purely coniferous trees is found in the region.

D) *Cultivated fields.* These are on light brown soils (inceptisols) covered with corn stalks, other crop debris and scattered patches of dry yellow grass less than 0.5 m tall.

E) *Grassy meadow.* Pasture land with short (<10 cm) grass. Trees cover less than 5% of the area.

F) *Shrubby grassland.* Former farmland composed primarily of 1–3 m tall deciduous shrubs and patches of 0.5–1.0 m tall yellow grass. Deciduous trees cover less than 10% of the area.

G) *Industrial.* The study site is an abandoned auto assembly plant. Its extensive dark roof is surrounded by large asphalt parking lots.

H) *Residential.* One and two story homes on ¼–½ acre lots with scattered trees and shrubbery. Roads and driveways are asphalted.

Key study sites for each surface type are shown in Fig. 1 under the same lettering.

Photographs in Fig. 2 show the muckland site (Fig. 1, site A) under deep snow cover and after the snow has melted. Partially flooded fields in the snowfree photo show a strong specular reflectance. Ninety percent of the upward flux recorded by the pyranometer comes from within the encircled area.

Table 3 provides information on flight times, solar zenith angle (SZA), average temperature, cloudiness and the range in atmospheric transmissivity during flights. It also shows the percentage of SW diffuse radiation and the percentage of SW insolation in the NIR, both measured on the ground prior to and following the flights. The majority of flights were taken within ±2 hours of noon with the SZA varying between 40 and 64°. All flights were made under overcast (0.9–1.0) or clear (0–0.1) sky conditions because the ground illumination of a studied scene can not be reliably determined under broken cloudiness. On cloudy days the transmissivities ranged between 15 and 65%; 65 to 100% of SW radiation was diffuse and 41% to 50% of the insolation was in the NIR. On clear days the transmissivities were 48–73%; 21–31% of the SW radiation was diffuse and 46–51% of the insolation was in the NIR.

3. Results

a. Key surface types

Time series of surface albedo at the key sites following the 11–12 February storm are shown in Fig. 3. The values are markedly heterogeneous when the surface is snow covered. They are much less so under snowfree conditions. Except for roads, parking lots, rooftops and, later in the period, steep south facing slopes, the ground remained fully snow covered until the flight of 25 February. By the 25th some bare soil and short grass became exposed on level

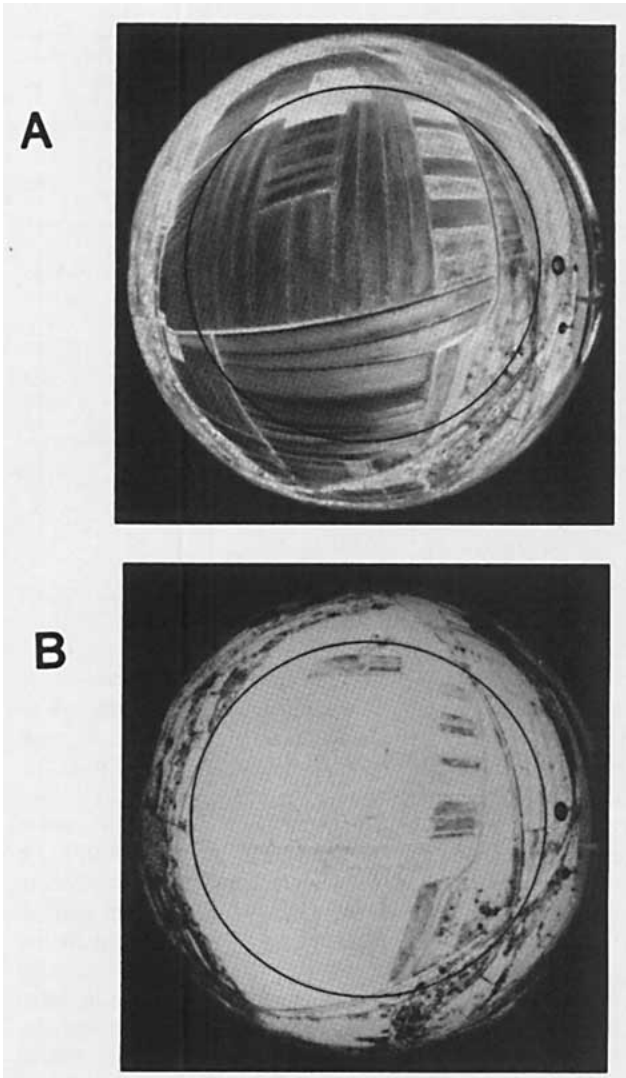

FIG. 2. (a) Mucklands in southeastern New York (cf. Fig. 1, site A) on 24 March 1983. The surface is partially flooded, resulting in some specular reflection from the dark soiled fields. Albedo is 0.07, visible reflectivity is 0.03 and near-infrared reflectivity is 0.10. (b) Snow-covered mucklands on 14 February 1983. Albedo is 0.79, VIS and NIR reflectivities are 0.89 and 0.68, respectively. North is towards the top in both photographs. 90% of the reflected signal is from the encircled area.

ground. By then the regional surfaces could be categorized as falling into one of two albedo classes; 1) fields (0.41–0.50) and 2) suburban and wooded (0.13–0.23) areas. Virtually all snow was gone by the 3 March flight.

Albedo over the mixed coniferous (curve C) and deciduous (B) stands and the residential site (H) decreased in a quasi-linear fashion. Albedo dropped at an accelerating rate over the mucklands (A) and other fields (D, E). The shrubby grassland (F) and industrial (G) sites exhibited a rapid initial drop of albedo followed by a relatively slow decrease. This was due to the exposure of low shrubs at F as the snow settled and fell off branches. At site G the change was due to the rapid melting of snow on rooftops and parking lots. The industrial site was snowfree approximately one week before the others.

Figures 4 and 5 show the progressive decrease of albedo and reflectivity over the muckland (A) and mixed forest (C) sites. Except during the snowstorm and for a few hours afterwards the coniferous canopy was snowfree. These two surfaces exhibit, respectively, the largest (0.72) and the smallest (0.10) ranges between snow-covered and snowfree albedo found in the region. Judging from published information, these ranges are close to the extremes which may be expected over continents. The albedo of uninterrupted snow cover on each of the flight dates is also shown in Figs. 4 and 5. The data were measured on the grounds of the Lamont–Doherty Geological Observatory (cf. Fig. 1). No soil or vegetation was exposed, nor was the measured surface shaded. The decreasing albedo of the mucklands parallels that of the ground snow measurements until 25 February, at which time the dark soil began to appear and the muckland albedo started falling faster than the snow albedo. The forest albedo decreased at a more regular rate, initially in response to the decreasing snow albedo,

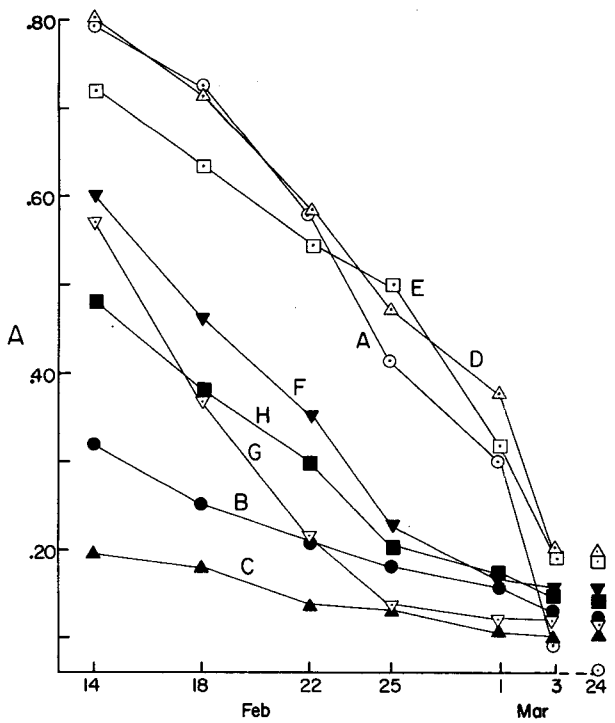

FIG. 3. Albedo (A) of major surface elements in southeastern New York and northern New Jersey under winterlike snowfree (24 March 1983) and a variety of snow covered (14 February–3 March 1983) conditions. The lettered curves correspond to locations marked on Fig. 1 and include (A) mucklands, (B) deciduous forest, (C) mixed coniferous forest, (D) cultivated field (E) grassy meadow, (F) shrubby grassland, (G) industrial and (H) residential.

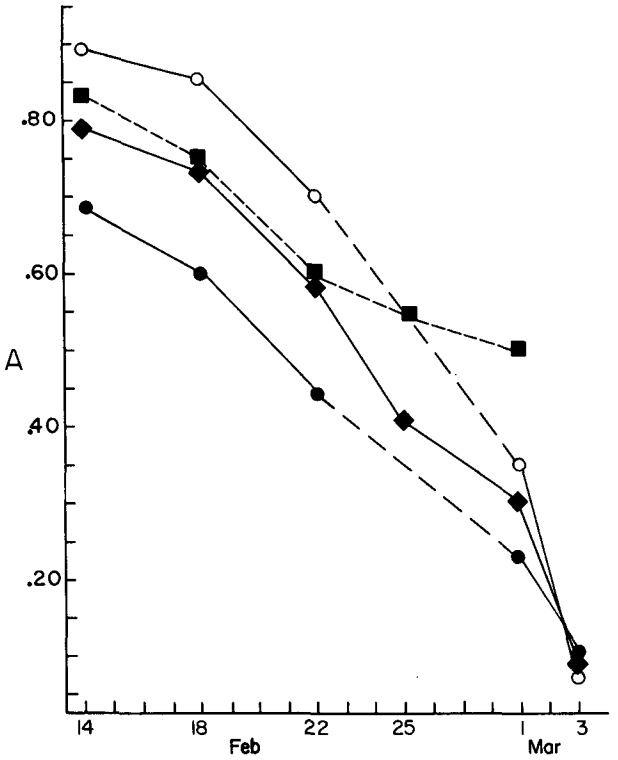

FIG. 4. Albedo and reflectivities (A) of the mucklands following the 11–12 February 1983 snowstorm: albedo (diamond), VIS reflectivity (open circle), NIR reflectivity (closed circle), ground measurements of snow albedo taken at Lamont (square).

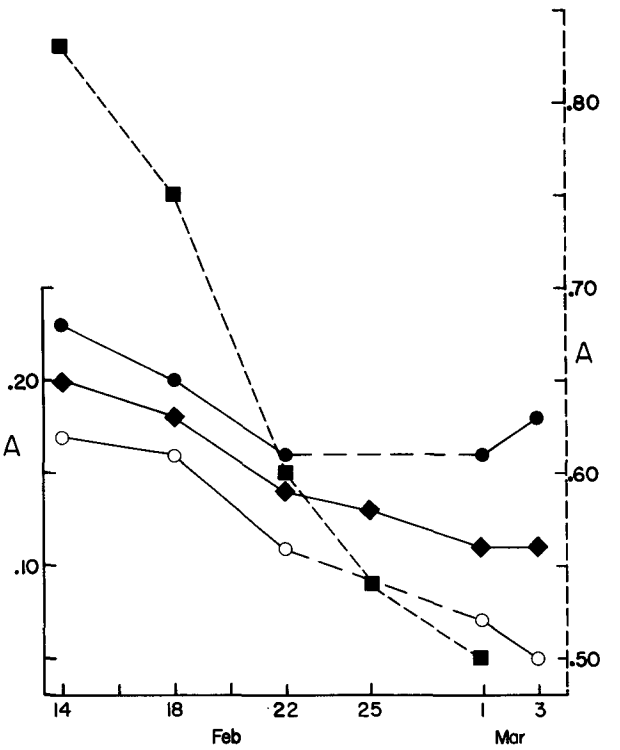

FIG. 5. Albedo and reflectivities of a mixed coniferous forest following the extreme snowfall. Symbols as in Fig. 4. The right axis shows the snow albedo; the other values are shown on the left axis.

and later in response to the exposure of snowfree patches on the forest floor.

Visible reflectivity (VIS) over the snow-covered mucklands is higher than in the NIR. The two converge as the snow ages, with the VIS eventually falling below the NIR once the site is virtually snowfree (3 March). The opposite occurs over the mixed forest: the VIS and NIR reflectivities diverge as the melt progresses. With most of the snow masked by the canopy, the high VIS reflectivity of the fully snow-covered forest floor brings the site VIS values to within 0.04 of the NIR reflectivity. With most of the snow gone on 3 March, the NIR reflectivity is 0.13 higher than the VIS value.

Between 1 and 3 March the NIR reflectivity of the mixed forest rose by 0.02. This is attributed to the sky being overcast on 1 March and clear on the 3rd. Very little snow was left on the ground on these two days. Narrowing of the range between NIR and VIS reflectivity under cloudy skies, with no change in albedo, was noted over all sites, whether they were snowfree or snow covered.

Table 4 lists the winter snowfree and maximum snow-covered albedos for sites A–H. Summer values averaged from two midday flights under clear skies in June and August are also shown. The winter snowfree values, averaged from two midday clear sky flights in January and March, are within 0.04 of summer albedos, with the exception of the mucklands, where dark peaty soil is exposed in winter but masked by the dense foliage of onion plants in summer. Other fields have lower summer albedos while wooded

TABLE 4. Annual range of surface albedos over major surface elements in southeastern New York and northern New Jersey. Summer values are averaged from 9 June and 3 August 1983 flights, except for the mucklands where 19 August 1982 data are used. Snowfree albedos representing winter conditions are averaged from 4 January and 24 March 1983 data. Maximum snow-covered values were measured on 14 February 1983. Letters correspond to sites discussed in Section 2.

Surface	Summer	Winter snow free	Maximum snow-covered
A mucklands	0.18	0.07	0.79
B deciduous forest	0.15	0.12	0.31
C mixed forest	0.14	0.10	0.20
D corn field	0.17	0.20	0.80
E meadow	0.16	0.19	0.72
F shrubby grassland	0.17	0.16	0.60
G factory	0.11	0.12	0.57
H residential	0.15	0.15	0.48

areas have higher summer values. There is relatively little winter-to-summer difference between the snow-free albedos of the industrial and residential areas.

The albedo of uninterrupted snow cover and the VIS and NIR reflectivities of the snow (cf. Table 1) show trends similar to theoretical models (e.g. Choudhury and Chang, 1978; Wiscombe and Warren, 1980; Warren and Wiscombe, 1980; Choudhury, 1981) with respect to changing grain size, wetness and depth. However, the VIS reflectivity is higher in the models than it is in nature. In the NIR it is not possible to directly compare measured results with the discrete spectral band values of the models.

b. Regional surfaces

Figures 6 and 7 show the relationship between visible and near-infrared reflectivity at 56 sites along the flight path. Data were gathered from all surface types present in the region both on 14 February under full snow cover and on 24 March when they were snowfree. In the snow-covered case, a linear relationship exists between the VIS and NIR reflectivities. With increasing proportions of vegetation masking the snow surface, both VIS and NIR reflectivities decrease, with the reflectivities becoming approximately equal over deciduous forests and VIS reflectivities falling below NIR values over mixed coniferous forests. The NIR reflectivities of all snow-free surfaces exceed VIS values, coming closest to unity at the industrial site (G) where little vegetation is present (Fig. 7, point G).

Snow depth alone is not the controlling variable of large-scale surface albedo (Lillesand *et al.*, 1982; Robinson and Kukla, 1982). Figure 8 substantiates this observation. In it, data from 26 sites along the flight path on February 22 are compared with those measured at the identical sites on February 10. On both dates the region was fully snow covered, mean

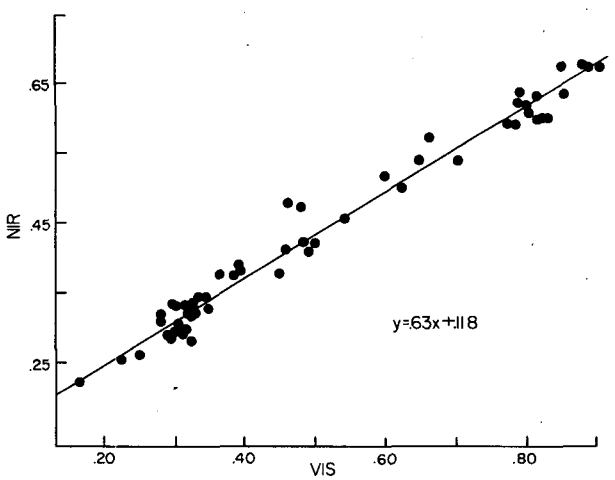

FIG. 6. VIS versus NIR reflectivities of a number of surfaces in southeastern New York and northern New Jersey under an approximately 50 cm deep snow cover. Data are from the 14 February 1983 flights. Correlation of the regression is 0.96.

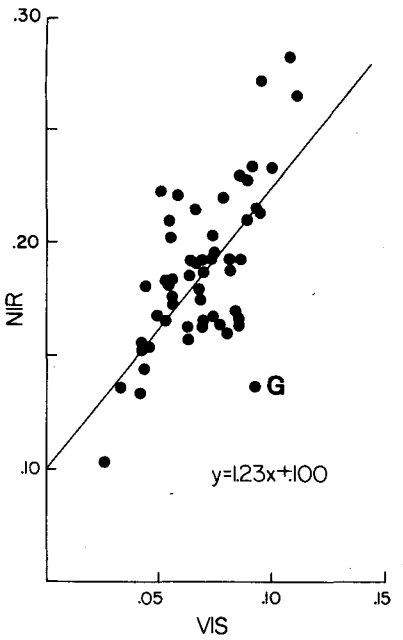

FIG. 7. VIS versus NIR reflectivities of a number of surfaces in southeastern New York and northern New Jersey under snowfree conditions. Data are from the 24 March 1983 flights. Correlation of the regression is 0.66. Point G is an industrial site (cf. Fig. 1, site G).

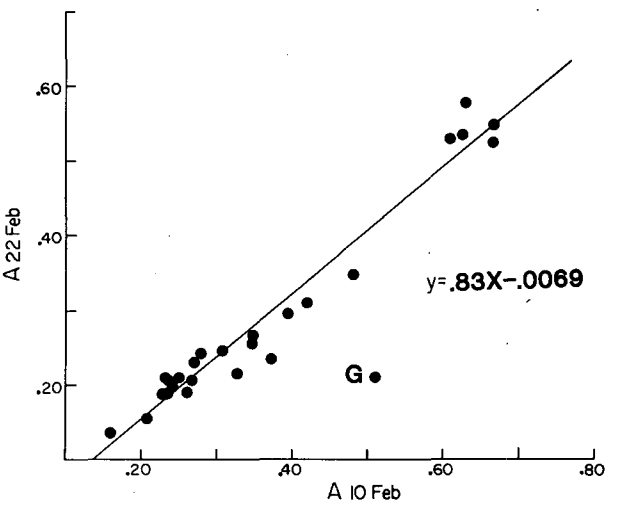

FIG. 8. Snow depth–age–albedo relationships. The albedo of a site on 10 February 1983 is plotted against the albedo of the identical site on 22 February 1983. Both days had clear skies and identical snow depths at forest and field test sites. Snow on 10 February was three days old and dry with an albedo of 0.78. Snow on 22 February was ten days old and wet with an albedo of 0.60. The regression equation has a correlation of 0.96. It does not include point G which is an industrial site (cf. Fig. 1, site G).

snow depth was approximately equal (13 cm), and skies were clear. The age and wetness of the snow both differed significantly between the two dates: it was 3 days old and dry on 10 February and 9 days old and wet on 22 February. In the former case the snow albedo was 0.78, in the latter 0.60. All large-scale albedo values were higher on the 10th, with differences between values on 10th and 22nd diminishing with increasing density of protruding vegetation. Only the industrial site (G), where snow of any depth remains for only a short time, does not fit the relationship (Fig. 8, point G).

In 20 fisheye aerial photographs taken between 14 February and 1 March, the fraction of exposed snow patches in the source area of 90% of the reflected flux was measured on an image processor. An exposed snow patch was defined as an area of full snow cover of at least 1 m^2, the nadir view of which was not masked or shaded by vegetation. Results were plotted against the normalized albedo (A_n) of the scene (Fig. 9). The latter value was derived by dividing the aerially-measured scene albedo by the ground-measured snow albedo on the given day. This allowed the impact of snowfree ground and masking vegetation on the scene albedo to be isolated from changes due to snow aging. Photographs of surfaces A and D–H (cf. Fig. 1) and of a deciduous stand with a small opening located near B were analysed. A consistent trend toward lower normalized albedo with decreasing snow exposure was observed, despite measurements having been made over a wide variety of surfaces and under full, as well as partial, snow cover conditions. The regression equation $y = 0.75x + 0.30$ is useful in estimating scene albedo when aerial measurements can not be made.

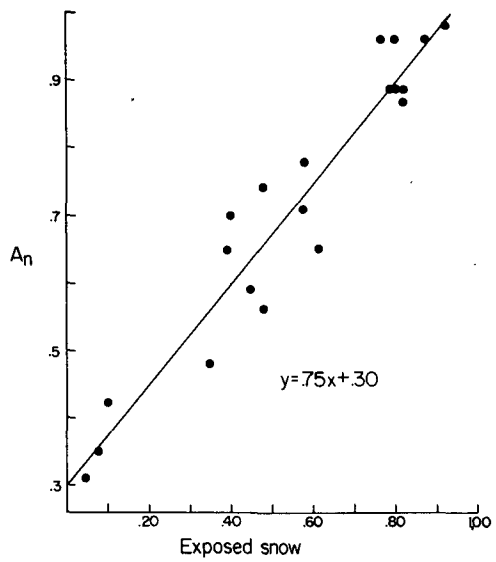

FIG. 9. Fraction of exposed snow patches plotted against the normalized scene albedo A_n. Exposed patches measured on an image processor from fisheye aerial photographs: A_n derived by dividing the aerially-measured albedo by the ground-measured snow albedo. For a variety of surfaces under the flight path with full and partial snow cover. Correlation of the regression is 0.96.

c. *Regional albedo*

Models of maximum surface albedo under snow over all of Rockland and Orange Counties (cf. Fig. 1) were constructed for the present and for several past periods using the measured albedos of the individual surface types and their areal distribution derived from land use records. At present the surface cover is 46% forest, 27% farm and open meadow and 27% commercial, residential or vacant (Robinson, 1984). Prior to the arrival of European settlers 95% of the region was forested, whereas in the late 19th century forests reached a low of 35%, with most of the remainder farm and open meadow. At present the maximum albedo under deep and fresh snow cover is 0.44. It was 0.31 before settlement and it reached 0.56 at the time of maximum deforestation.

The present maximum albedo agrees well with a maximum of 0.42 derived from satellite data over this region (Robinson, 1984; Robinson and Kukla, 1985) and is close to the regional albedo reported by Kung *et al.* (1964) for January snow cover 13 cm or deeper and to January values reported by Kondratyev *et al.* (1981). It should be realized, however, that in winter over much of the middle latitudes the snow cover is frequently aged, shallow and/or discontinuous. As is illustrated in this report, monthly means should be considerably lower than those for fresh cover.

4. Conclusions

Surface albedo and spectral reflectivities were monitored over typical middle latitude surfaces during the dissipation of a 50 cm deep snow cover. Data gathered include the maximum and minimum winter albedos that can be expected in the region. Throughout the period, daytime temperatures were above freezing with no significant rain or snowfall. As a result, a time series of surface albedo of a continuously dissipating snowpack was obtained. A wide range in the albedo of different surface types was observed under full snow cover. It narrowed considerably under snowfree conditions. Among the surfaces monitored were those exhibiting close to the largest (0.72) and smallest (0.10) ranges between snow-covered and snowfree albedo expected over land. Albedo and reflectivity changed during the melt as a result of variations in vegetation density, snow depth, granularity and wetness. Visible reflectivities were higher than near-infrared values over snow-covered fields and shrublands. Visible and NIR values were approximately equal over deciduous forest and NIR values were higher over mixed coniferous forests. Near-

infrared reflectivities exceeded VIS values in all snow-free cases.

The results should be useful in improving snow albedo parameterizations in climate models, in verifying satellite-derived albedo estimates, and in assessments of man's impact on winter climate.

Acknowledgments. Thanks to J. Gavin for assisting in the acquisition of aerial data and for reading the manuscript and to J. Hays, G. Jacoby, J. Otterman and A. Robock for reading the manuscript. This work was funded by NSF Grant ATM82-00863.

REFERENCES

Barry, R. G., and R. E. Chambers, 1966: A preliminary map of summer albedo over England and Wales. *Quart. J. Roy. Meteor. Soc.*, **92,** 543–548.

Bauer, K. G., and J. A. Dutton, 1962: Albedo variations measured from an airplane over several types of surface. *J. Geophys. Res.*, **67,** 2367–2376.

Berglund, E. R., and A. C. Mace Jr., 1972: Seasonal albedo of black spruce and sphagnum-sedge bog cover types. *J. Appl. Meteor.*, **11,** 806–812.

Choudhury, B., 1981: Spectral albedos of midlatitude snowpacks. NASA Tech. Memo. 83858, 37 pp.

——, and A. T. C. Chang, 1978: Two-stream theory of spectral reflectance of snow. NASA Tech. Memo. 79639, 16 pp.

Eaton, F. D., and I. Dirmhirn, 1979: Reflected irradiance indicatrices of natural surfaces and their effect on albedo. *Appl. Opt.*, **18,** 994–1008.

Federer, C. A., 1971: Solar radiation absorption by leafless hardwood forests. *Agric. Meteor.*, **9,** 3–20.

Henderson-Sellers, A., and M. Wilson, 1983: Surface albedo data for climatic modeling. *Rev. Geophys. Space Phys.*, **21,** 1743–1778.

Jurik, T. W., and D. M. Gates, 1983: Albedo following fire in a northern hardwood forest. *J. Climate Appl. Meteor.*, **22,** 1733–1737.

Kondratyev, K. Y., V. I. Korzov, V. V. Mukhenberg and L. N. Dyachenko, 1981: The shortwave albedo and the surface emissivity. *JSC Study Conf. on Land Surface Processes in Atmospheric General Circulation Models,* Greenbelt, MD, World Climate Research Programme, 463–514.

Kung, E. C., R. A. Bryson and D. H. Lenschow, 1964: Study of a continental surface albedo on the basis of flight measurements and structure of the earth's surface cover over North America. *Mon. Wea. Rev.*, **22,** 543–564.

Lillesand, T. M., D. E. Meisner, A. LaMois Downs and R. L. Deuell, 1982: Use of GOES and TIROS/NOAA satellite data for snow-cover mapping. *Photogramm. Eng. Remote Sens.*, **48,** 251–259.

Matthews, E., 1983: Global vegetation and land use: New high-resolution data bases for climate studies. *J. Climate Appl. Meteor.*, **22,** 474–487.

McFadden, J. D., and R. A. Ragotzkie, 1967: Climatological significance of albedo in central Canada. *J. Geophys. Res.*, **72,** 1135–1143.

O'Neill, A. D. J., and D. M. Gray, 1973: Spatial and temporal variations of the albedo of prairie snowpack. *Role of Snow and Ice in Hydrology. Proc. Banff Symposia,* Vol. 1, UNESCO/WMO/IAHS 176–186.

Ramanathan, V., M. S. Lian and R. D. Cess, 1979: Increased atmospheric CO_2: Zonal and seasonal estimates of the effect on the radiation energy balance and surface temperature. *J. Geophys. Res.*, **84,** 4949–4958.

Robinson, D. A., 1984: Anthropogenic impact on winter surface albedo. Doctoral thesis, Columbia University, 394 pp.

——, and G. Kukla, 1982: Remotely sensed characteristics of snow covered lands. *1982 Int. Geosci. Remote Sens. Symp. Digest,* W. Keydel, Ed., *IEEE,* WA-1, 2.1–2.9.

——, and G. Kukla, 1985: Maximum surface albedo of seasonally snow covered lands in the Northern Hemisphere. *J. Climate Appl. Meteor.*, **24,** (4, in press).

Robock, A., 1980: The seasonal cycle of snow cover, sea ice and surface albedo. *Mon. Wea. Rev.*, **108,** 267–285.

——, 1983: Ice and snow feedbacks and the latitudinal and seasonal distribution of climate sensitivity. *J. Atmos. Sci.*, **40,** 986–997.

Rockwood, A. A., and S. K. Cox, 1978: Satellite inferred surface albedo over Northwestern Africa. *J. Atmos. Sci.*, **35,** 513–522.

Taylor, V. R., and L. L. Stowe, 1984: Reflectance characteristics of uniform earth and cloud surfaces derived from Nimbus-7 ERB. *J. Geophys. Res.*, **89,** 4987–4996.

Warren, S. G., and W. J. Wiscombe, 1980: A model for the spectral albedo of snow. Part II: Snow containing atmospheric aerosols. *J. Atmos. Sci.*, **37,** 2734–2745.

Wiscombe, W. J., and S. G. Warren, 1980: A model for the spectral albedo of snow. Part I: Pure snow. *J. Atmos. Sci.*, **37,** 2712–2733.